Supplementary Information

Enhancing the electrical transport properties of two-dimensional semiconductors through interlayer interactions

Qinghang Tang [a,b], Shihao Han [a], Mingjia Yao [b], David J. Singh [c], Jinyang Xi [b,d], Huijun Liu [a,*], Jiong Yang [b,d,†]

[a] Key Laboratory of Artificial Micro- and Nano-Structures of Ministry of Education and School of Physics and Technology, Wuhan University, Wuhan 430072, China

[b] Materials Genome Institute, Shanghai University, Shanghai, 200444, China

[c] Department of Physics and Astronomy, University of Missouri, Columbia, MO 65211, USA

[d] Zhejiang Laboratory, Hangzhou, Zhejiang 311100, China

The Test of Effective Thickness Conversion

For the results from the constant relaxation time approximation (CRTA), the carrier concentration, electrical conductivity and power factor need to be rescaled by a factor of *c/h*, and the electronic fitness function (EFF) should be normalized by multiplying $(c/h)^{1/3}$. In the case of constant electron–phonon coupling approximation (CEPCA), the relaxation time τ is proportional to the volume *V*. Thus, except for the carrier concentration multiplied by *c/h*, other transport coefficients do not need to be converted.

We give an example to show the calculated results of the electrical transport coefficients where the effective thickness is taken into consideration. We randomly select a system (Sn_2Se_2) from 166 semiconductor bilayers, whose initial interlayer distance is set to be 10 Å (bilayer(10 Å)), and calculate its electrical transport properties. In fact, bilayer(10 Å) simulates the absence of interlayer interactions, and its essence is consistent with the monolayer. As can be seen in Fig. S1, the band structure of the Sn_2Se_2 bilayer(10 Å) is the same as the corresponding monolayer, except that the degeneracy of each band is doubled. By considering the *h*, the electrical

* Author to whom correspondence should be addressed. Electronic mail: phlhj@whu.edu.cn

† Author to whom correspondence should be addressed. Electronic mail: jiongy@t.shu.edu.cn

transport coefficients of bilayer(10 Å) are consistent with those of monolayer under both CRTA and CEPCA (seen in Fig. S2 and S3). The above results indicate the rationality of considering the effective thickness conversion.

Furthermore, a carrier concentration needs to be determined to compare the transport coefficients in high-throughput screening. Among the 166 semiconductor bilayers, the maximum and minimum h of the corresponding monolayers are 11.25 Å and 3.2 Å, respectively. After converting the carrier concentration of the 2D monolayer ($1.0 \times 10^{11} \sim 1.0 \times 10^{14}$ cm^{-2})[1–2] according to these two extreme h, the carrier concentration ranges can be obtained as $8.89 \times 10^{17} \sim 8.89 \times 10^{20}$ cm^{-3} and $3.12 \times 10^{18} \sim 3.12 \times 10^{21}$ cm^{-3}, respectively. Therefore, the moderate value of 5.0×10^{19} cm^{-3} at the intersection of these two carrier concentrations was selected in following electrical transport coefficients screening.

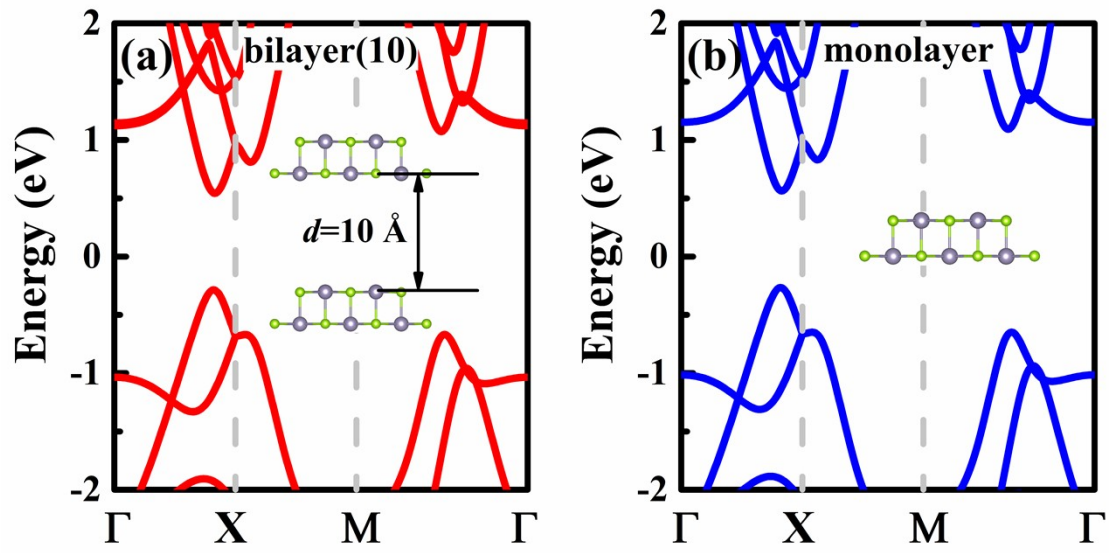

Fig. S1 The band structure of Sn_2Se_2 (a) bilayer(10 Å) and (b) monolayer counterpart, the inset is the corresponding crystal structure.

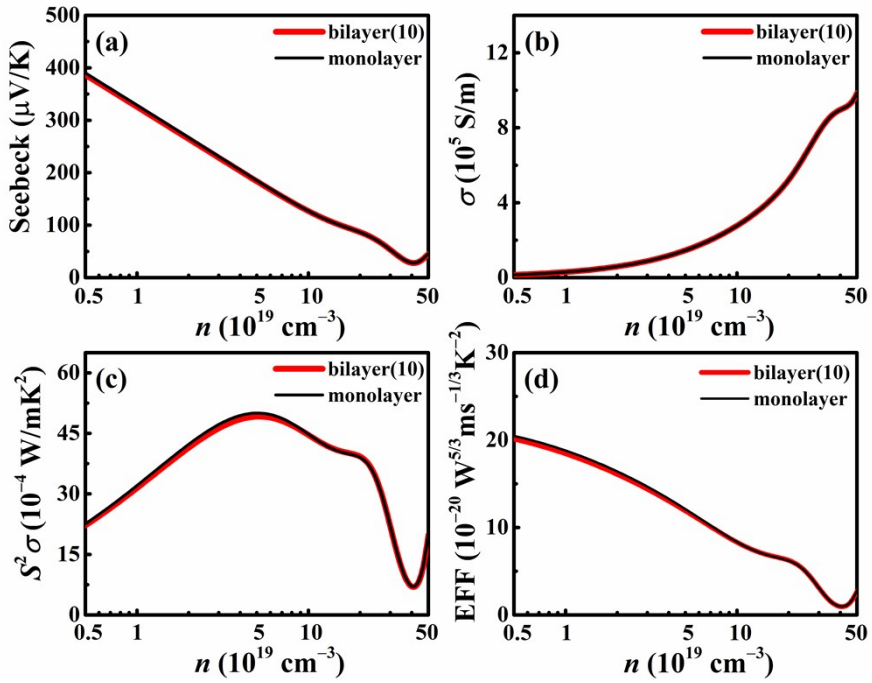

Fig. S2 Under CRTA, the electrical transport coefficients of Sn_2Se_2 monolayer and bilayer(10 Å) are compared after considering the effective thickness, (a) the Seebeck coefficient, (b) the electrical conductivity, (c) the power factor, (d) the electronic fitness function.

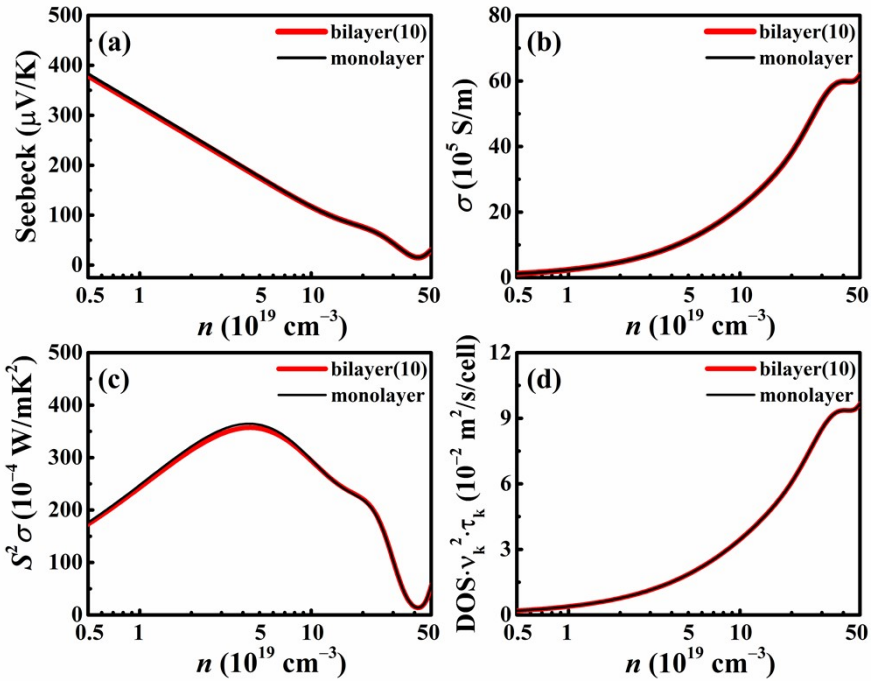

Fig. S3 Under CEPCA, the electrical transport coefficients of Sn_2Se_2 monolayer and bilayer(10 Å) are compared after considering the effective thickness, (a) the Seebeck coefficient, (b) the electrical conductivity, (c) the power factor, (d) the transport distribution function.

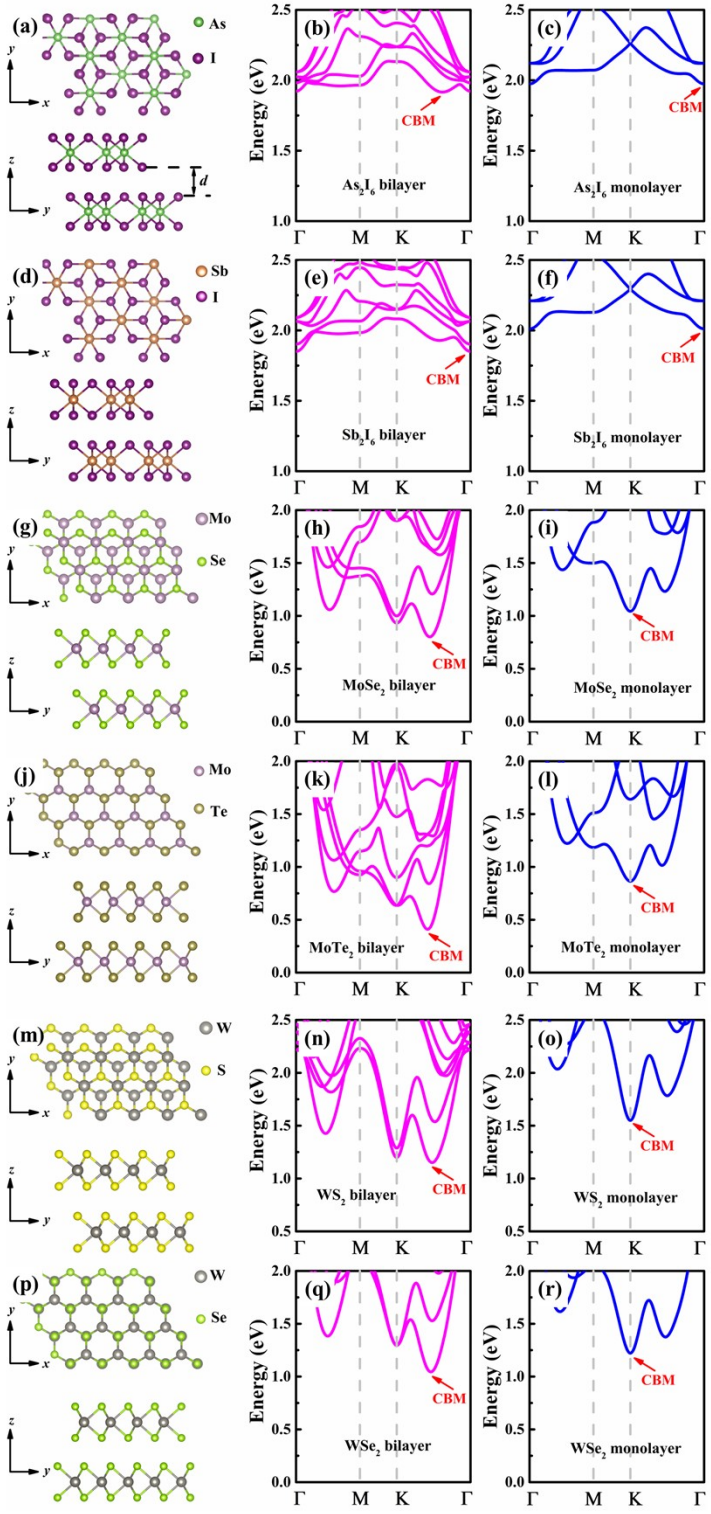

Fig. S4 The crystal structures and the band structures of six bilayer systems. For comparison, the results of monolayer counterparts are also shown: (a-c) As_2I_6, (d-f) Sb_2I_6, (g-i) $MoSe_2$, (j-l) $MoTe_2$, (m-o) WS_2, (p-r) WSe_2.

Fig. S5. The phonon dispersion relations of (a) the As_2I_6 bilayer, (b) the Sb_2I_6 bilayer, and (c) $MoSe_2$ bilayer.

Fig. S6. The *ab initio* molecular dynamics results of the average values of (a) the As–I distances in As_2I_6 bilayer, (b) the Sb–I distance in Sb_2I_6 bilayer, and (c) the Mo-Se distance in $MoSe_2$ bilayer at 300 K. The dashed line indicates a 5% deviation from the equilibrium distance.

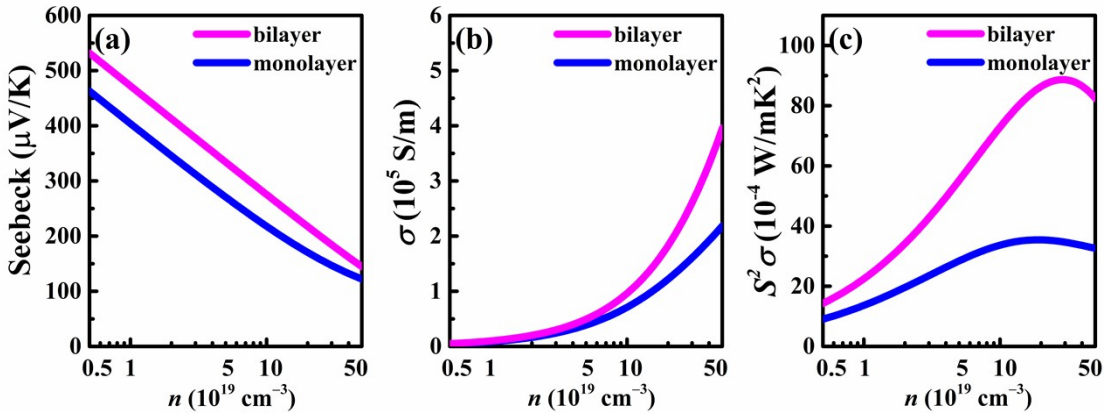

Fig. S7 (a) The Seebeck coefficient, (b) the electrical conductivity, and (c) the power factor of the As_2I_6 bilayer and corresponding monolayer at 300 K.

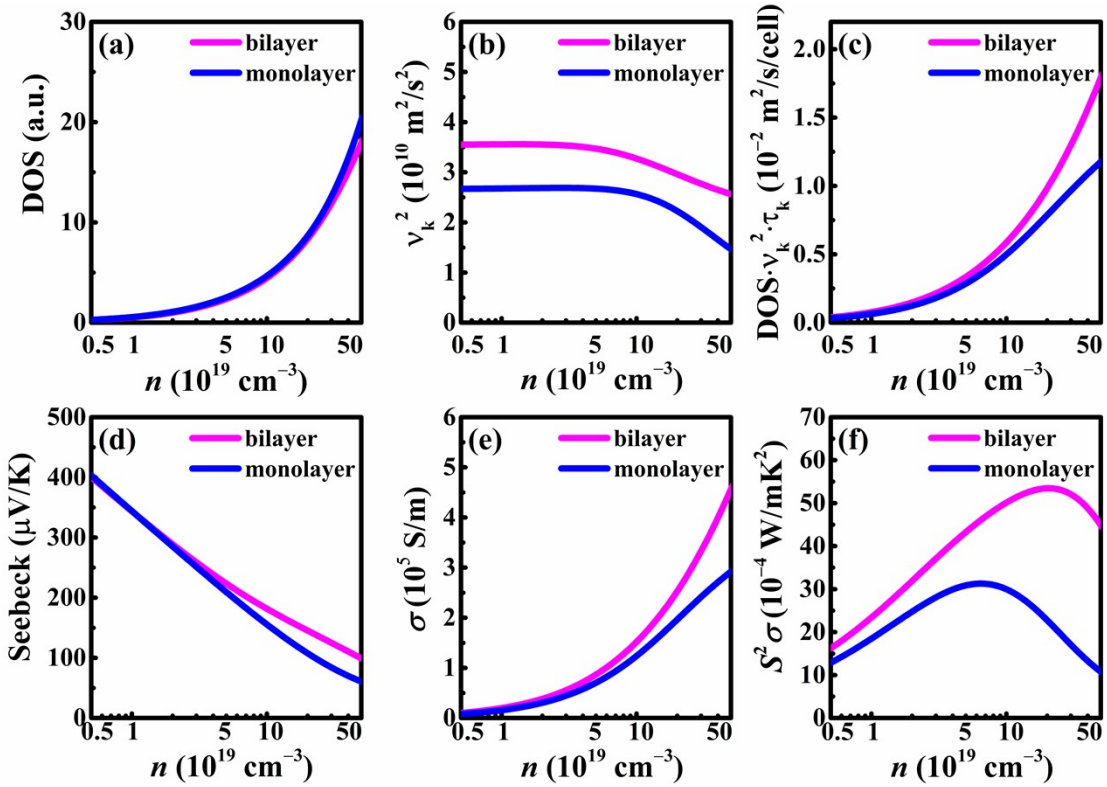

Fig. S8 The electrical transport coefficients of Sb_2I_6 bilayer as a function of carrier concentration at 300 K. (a) The density of states, (b) the square of electronic group velocity, (c) the transport distribution function, (d) the Seebeck coefficient, (e) the electrical conductivity, and (f) the power factor.

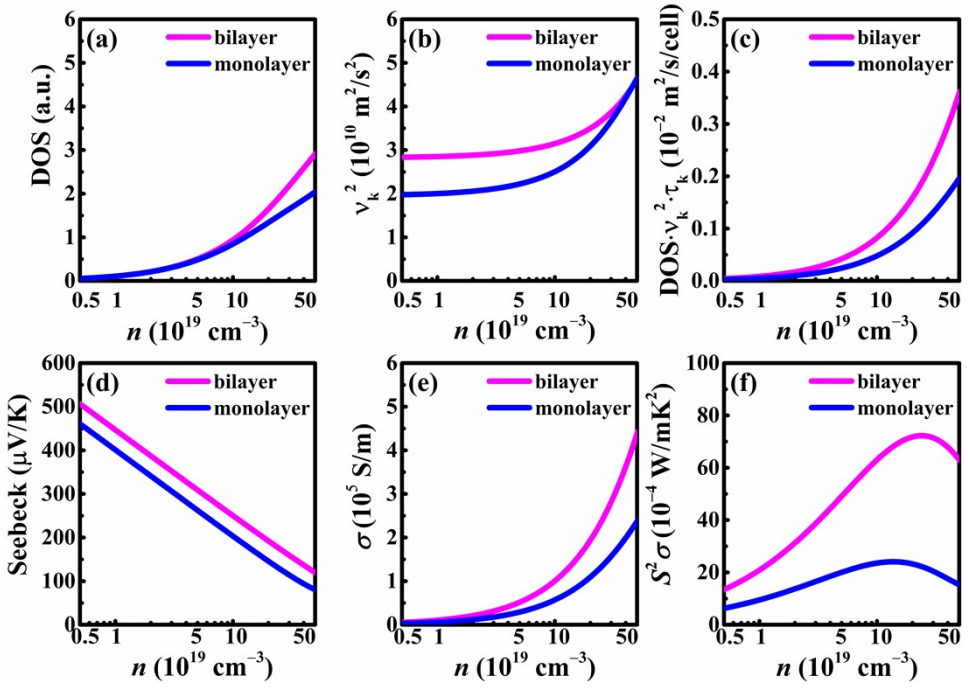

Fig. S9 The electrical transport coefficients of $MoSe_2$ bilayer as a function of

carrier concentration at 300 K. (a) The density of states, (b) the square of electronic group velocity, (c) the transport distribution function, (d) the Seebeck coefficient, (e) the electrical conductivity, and (f) the power factor.

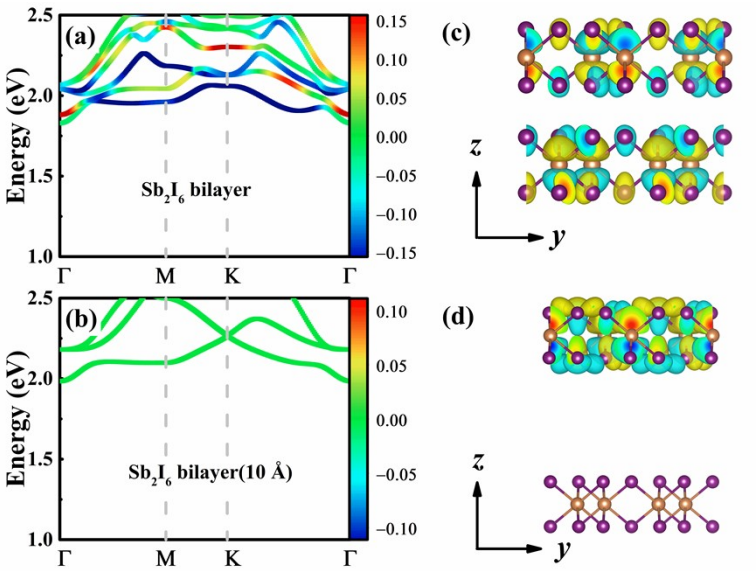

Fig. S10 The band-resolved COHPs and wave functions of Sb_2I_6 system. The band-resolved COHPs between the top and bottom layers for the Sb_2I_6 (a) bilayer, and (b) bilayer(10 Å). The wave functions at the CBM for the Sb_2I_6 (c) bilayer, and (b) bilayer(10 Å).

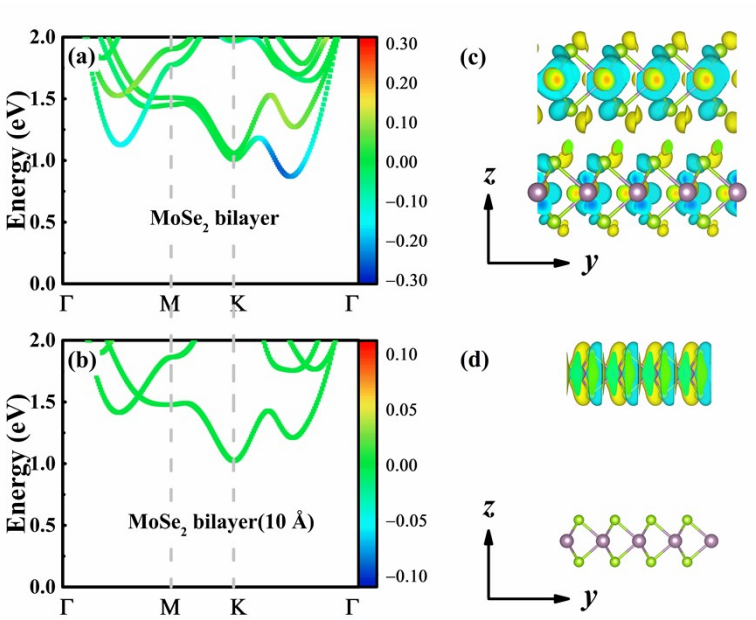

Fig. S11 The band-resolved COHPs and wave functions of $MoSe_2$ system. The band-resolved COHPs between the top and bottom layers for the $MoSe_2$ (a) bilayer, and (b) bilayer(10 Å). The wave functions at the CBM for the $MoSe_2$ (c) bilayer, and (b) bilayer(10 Å).

Table S1. The binding energy and electrical transport coefficients of 34 bilayer systems with power factors larger than those of monolayers.

		Bilayer			monolayer		
	E_b (eV/Å^2)	σ (10^5 S/m)	S (μV/K)	$S^2\sigma$ (10^{-4} W/mK^2)	σ (10^5 S/m)	S (μV/K)	$S^2\sigma$ (10^{-4} W/mK^2)
$Ag_1Er_1P_2Se_6$	–22.88	1.11	300.26	99.71	0.86	318.85	86.98
$Ag_1P_2Sc_1Se_6$	–21.04	0.68	323.70	71.16	0.35	374.64	48.63
$Ag_1P_2Se_6Tm_1$	–21.61	1.42	285.36	115.94	0.83	321.74	85.98
As_2I_6	–16.28	0.49	335.62	54.70	0.39	270.46	28.45
B_1I_3	–11.03	0.40	334.17	44.13	0.29	376.62	41.46
B_1N_1	–16.96	0.48	396.72	75.84	0.21	430.33	38.66
$Br_2Hf_2N_2$	–20.77	2.56	250.03	159.80	2.49	251.01	157.23
$Br_2Ho_2O_2$	–17.92	0.90	269.29	65.52	0.88	270.17	64.37
$Br_2N_2Zr_2$	–20.73	2.76	239.47	158.37	2.74	238.80	155.99
Cl_2Zr_1	–20.65	0.55	325.62	58.84	0.24	416.22	41.70
Ga_1N_1	–14.33	42.80	147.11	926.18	19.36	210.64	859.19
Ga_1P_1	–75.04	26.20	65.61	112.79	6.09	133.46	108.43
Ga_2S_2	–20.13	1.45	281.42	114.46	4.40	138.49	84.42
Ge_1Te_1	–25.02	5.10	239.04	291.31	2.87	311.59	278.28
Ge_1Te_1	–24.95	4.99	241.49	291.35	3.01	306.18	281.91
$H_2Mg_1O_2$	–4.22	4.92	182.75	164.42	2.59	243.95	154.19
$H_2Mg_2O_3$	–7.07	4.96	160.77	128.27	2.55	217.39	120.39
$H_2Ni_1O_2$	–4.49	5.78	162.38	152.52	3.15	198.96	124.62
H_2Si_2	–3.11	5.16	324.87	544.87	5.10	324.73	537.88
I_3P_1	–13.65	1.75	267.90	125.47	0.78	357.54	99.34
I_6Sb_2	–14.02	0.87	222.99	43.36	0.70	209.31	30.88
Mo_1S_2	–32.11	0.39	342.99	45.65	0.42	254.05	26.94
Mo_1Se_2	–34.25	0.51	308.85	49.09	0.29	263.44	19.96
Mo_1Te_2	–38.50	0.72	282.01	57.50	0.30	263.65	21.01
$O_{18}Te_8$	–32.83	1.49	238.49	84.82	0.74	328.19	79.59
Pt_1S_2	–32.57	1.38	298.59	123.10	1.06	336.61	119.76
S_2W_1	–33.82	0.59	305.85	55.71	0.58	221.64	28.45
Se_2W_1	–36.34	0.89	279.14	69.49	0.45	230.44	23.87
Ba_1O_2	–46.30	2.20	164.99	59.77	1.10	227.14	56.70
$Cl_2N_2Th_2$	–51.87	5.26	129.88	88.78	1.64	206.66	70.07
$H_2I_2Sr_2$	–18.42	1.52	216.18	71.21	1.09	166.30	30.05
$I_2N_2Th_2$	–26.33	1.97	149.49	44.02	1.31	175.52	40.38
$Li_2Rb_2S_2$	–32.67	3.35	194.84	127.13	2.60	197.56	101.61
O_2Sn_2	–38.87	11.98	183.49	403.26	0.70	370.55	96.40

Table S2. The ratio of the electrical transport coefficients between the bilayer and the corresponding monolayer at the electron concentration of 5.00×10^{19} cm^{-3} at 300 K.

	$\frac{S_{bilayer}}{S_{monolayer}}$	$\frac{\sigma_{bilayer}}{\sigma_{monolayer}}$	$\frac{S^2\sigma_{bilayer}}{S^2\sigma_{monolayer}}$	$\frac{\tau_{bilayer}}{\tau_{monolayer}}$	$\frac{DOS_{bilayer}}{DOS_{monolayer}}$	$\frac{(v_k^2)_{bilayer}}{(v_k^2)_{monolayer}}$
WS_2	1.38	1.03	1.96	1.04	1.16	0.82
WSe_2	1.21	1.98	2.91	1.47	1.09	1.20
$MoTe_2$	1.07	2.39	2.74	1.31	0.99	1.79

Table S3. The electrical transport coefficients of As_2I_6 under different layers.

	DOS	**(v_k^2) (10^{10} m^2/s^2)**	**σ (10^5 S/m)**	**S (μV/K)**	**$S^2\sigma$ (10^{-4} W/mK^2)**
Monolayer	0.64	1.53	0.39	270.46	28.45
Bilayer	0.61	1.93	0.49	335.62	54.70
3L	0.60	2.17	0.57	289.41	47.93
4L	0.57	2.30	0.61	262.81	41.96
5L	0.57	2.39	0.62	254.66	40.51
6L	0.57	2.44	0.64	247.81	39.13
7L	0.57	2.48	0.65	249.52	40.36

References

(1) D. A. Schmidt, T. Ohta and T. E. Beechem, *Phys. Rev. B*, 2011, **84**.

(2) B. Zhu, Q. Chen, S. Jiang, M. Holt, W. Zhu, D. Akinwande and L. Tao, *InfoMat*, 2021, **3**, 271–292.